Thermal Network Model of High-Power Dry-Type Transformer Coupled With Electromagnetic Loss

Yifan Chen, Qingxin Yang, Changgeng Zhang, Yongjian Li, and Xinghan Li

State Key Laboratory of Reliability and Intelligence of Electrical Equipment, Hebei University of Technology, Tianjin 300130, China

Hebei Province Key Laboratory of EFEAR, Hebei University of Technology, Tianjin 300130, China

Based on thermoelectric analogy method, a thermal network model coupled with electromagnetic loss is presented. According to the actual structure of dry-type transformer windings, an accurate thermal network is established. Considering the distribution characteristics of heat source along the cooling ducts inside the dry-type transformer, the thermal parameters such as heat flux and convective heat transfer coefficients are calculated by finite element method (FEM) analysis and computational fluid dynamics (CFD). Based on the temperature rise experiment, the hottest spot located at the top of the outmost high-voltage (HV) winding is 151.8 °C, which verified the correctness of thermal network model.

Index Terms— **Computational fluid dynamics (CFD), convective heat transfer coefficient, dry-type transformer, FEM, thermal network method.**

I. Introduction

DRY-TYPE transformer is widely used for their high safety performance and environmental protection. The windings of dry-type transformers are poured by epoxy resin as a whole. With poor heat dissipation performance and uneven loss distribution, high-power dry-type transformer is easily damaged by inter-turn short circuit for insulation aging and local overheating [1], [2]. Therefore, to extend equipment life, the evaluation of the temperature distribution for dry-type transformers has profound meaning [3]. At present, the methods to predict the temperature distribution of electrical equipment mainly include finite element method (FEM) [4], computational fluid dynamics (CFD) [5], [6], and lumped parameter thermal network method (LPTN) [7]. For many complex problems, accurate results can be obtained by the extremely fine mesh of FEM and CFD. However, the extremely fine mesh also brings large-scale computation. Based on the theory of thermo-electricity analogy, the LPTN method simulates the path of heat transfer by thermal network. Compared with FEM and CFD, the LPTN method has the advantages of having clear physical meaning and fast calculation speed. However, the traditional LPTN method cannot accurately describe the complex boundary conditions under natural convection condition, which results in poor calculation precision.

In this article, a thermal network model of dry-type transformer coupled with FEM and CFD is presented. First, the transformer windings are divided into 11 regions for the distribution characteristics of heat sources and heat dissipation conditions. Each region is represented by one network node. The high-voltage (HV) wire is taken as a subunit for fine modeling so as to consider the influence of thin insulating paint on heat dissipation. Then, the eddy loss distribution of transformer low-voltage (LV) windings is calculated by FEM, while the corresponding temperature and velocity field distributions are calculated by coupling with CFD. The loss calculated by FEM and the convective heat transfer coefficient (h) by CFD are taken as the input of the thermal network for calculation of thermal parameters. Finally, the effectiveness of the method is verified by temperature rise experiment, which can provide a reference for rapid temperature calculation of dry-type transformer.

Manuscript received 24 March 2021; revised 11 July 2021; accepted 24 July 2021. Date of publication 11 August 2021; date of current version 24 October 2022. Corresponding author: C. Zhang (e-mail: changgeng.zhang@hebut.edu.cn).

Color versions of one or more figures in this article are available at https://doi.org/10.1109/TMAG.2021.3104090.

Digital Object Identifier 10.1109/TMAG.2021.3104090

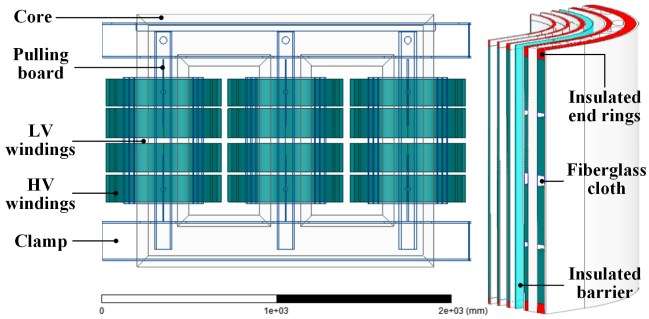


Fig. 1. Dry-type transformer model.

II. Establishment of Thermal Network Model

A. Structure of Dry-Type Transformer

A three-phase 2500 kVA dry-type transformer is shown in Fig. 1, whose windings are composed of LV foil windings and HV segmented layer windings. Separated by the insulating paper, two layers of LV windings are in parallel as one turn. Consisted of enameled rectangular copper wires, the HV-segmented layer windings can be divided into four sections, which are insulated by fiberglass cloth.

B. Topology of Thermal Network Model

The cooling ducts of the dry-type transformer are vertical annulus-shaped, in which the distribution characteristics of heat source and cooling conditions of LV and HV windings are quite different from each other. In the established thermal network model, the LV and HV windings are divided into 11 regions according to the distributions of their heat source.

0018-9464 © 2021 IEEE. Personal use is permitted, but republication/redistribution requires IEEE permission.
See https://www.ieee.org/publications/rights/index.html for more information.

Authorized licensed use limited to: Hebei University of Technology. Downloaded on November 17,2022 at 09:36:45 UTC from IEEE Xplore. Restrictions apply.

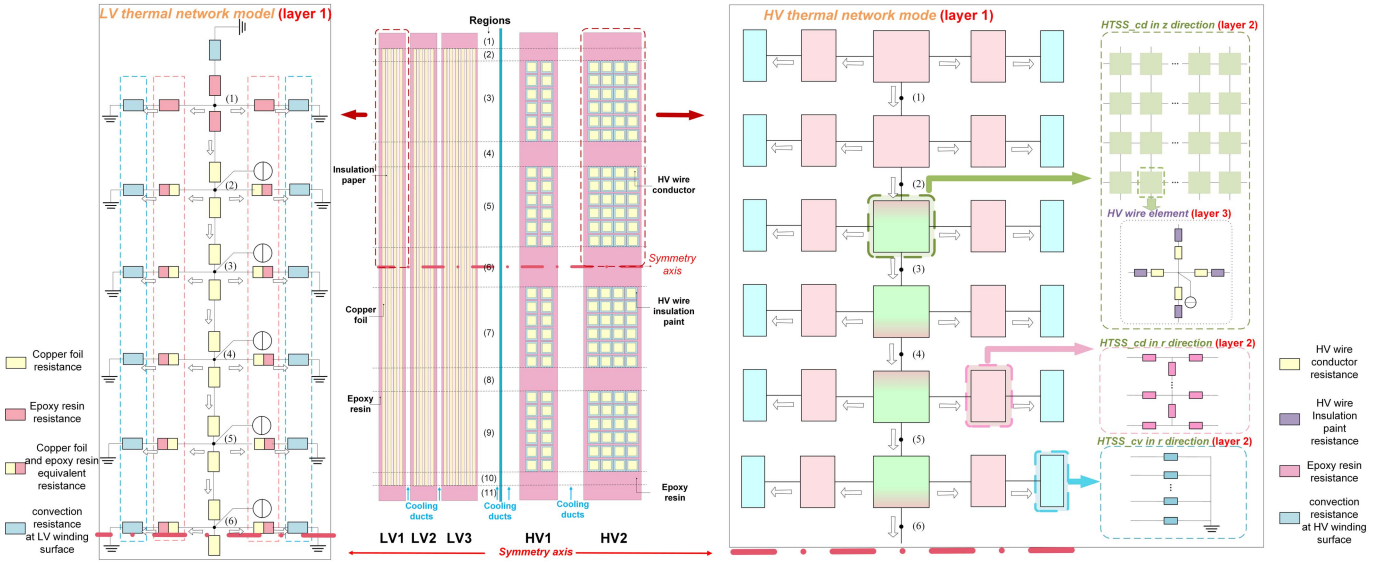


Fig. 2. Structure of the thermal network model. (a) Thermal network detailed structure of LV1. (b) Divided regions and corresponding nodes. (c) Thermal network detailed structure of HV2.

The temperature in each region is represented by one node. Based on the symmetry of the windings, the half thermal network structure is shown in Fig. 2. The established thermal network model can be extended to various power transformers with the same determined structure.

For LV windings, the heat source at the end position is larger than that at the middle. Beyond that, the change in heat source distribution and material properties along the axial direction is limited. Except for the winding end made of insulation material, the remaining LV windings are made of copper foil. Connected by resistance directly, the thermal network structure of LV1 upper part is shown in Fig. 2(a), in which nodes 1–6 correspond to regions 1–6 in Fig. 2(b). The other half of the thermal network has the same structure.

On account of the HV windings' structure shown in Fig. 2(b), the heat sources' distribution and material properties fluctuate along the axial direction. The method of homogenizing distributed thermal resistance in all insulation layers to the lumped thermal resistance of the outermost layer would cause calculation error. The thermal network of HV2 is multi-layered and the thermal conductivity resistances are shown in Fig. 2(c). There is a heat transfer subsystem of conduction (HTSS_cd) in the axial direction between two nodes, which consists of the subunit of HV copper wire. The axial conduction thermal resistances of the epoxy resin between the HV windings segments are considered. In the radial direction, the HTSS_cd is a collection of epoxy resin resistances. The heat transferred to the solid wall surface is eventually dissipated to the surrounding environment through the heat transfer subsystem of convection (HTSS_cv). The thermal network models of LV2, LV3, and HV1 can be inferred in the same way.

III. Finite Element and CFD Simulation Analysis

The following assumptions to build an FEM model of dry-type transformer are summarized.

1) The heat dissipation condition of each phase winding is the same, so only a single-phase winding need to be calculated.
2) The influences of the structure of fan, strut, and pull plate on heat dissipation are ignored.
3) The eddy current loss in the HV windings is ignored.

A. Eddy Current Loss Calculation by FEM

The winding loss consists of direct current (dc) loss and eddy loss. dc loss is generated from the winding resistance under dc excitation, whose value is proportional to the square of load current. The leakage magnetic field causes the induced eddy current, which leads to uneven loss distribution in the LV windings. The corresponding governing equations for the eddy current region are as follows:

$$\nabla \times \left(\frac{1}{\mu}\nabla \times \boldsymbol{A}\right) = -(\boldsymbol{J}_s + \boldsymbol{J}_e) \tag{1}$$

$$\boldsymbol{J}_e = -\sigma_e\left(\frac{\partial \boldsymbol{A}}{\partial t} + \nabla\varphi\right) \tag{2}$$

$$\nabla \cdot (\boldsymbol{J}_s + \boldsymbol{J}_e) = 0 \tag{3}$$

where $\boldsymbol{A}$ is the magnetic vector potential, φ is the electric scalar potential, μ is the magnetic permeability tensor, $\boldsymbol{J}_s$ is the source current density of the conductor, $\boldsymbol{J}_e$ is the eddy current density induced by leakage flux, and σ_e is the electric conductivity.

As shown in Fig. 3, the eddy current density at the end position can reach 1.5–2.5 times at the middle, which would lead to local overheating of the transformer. Therefore, the uneven loss distribution caused by leakage magnetic field should be taken into account when calculating the temperature rise of the thermal network model. The calculation results of d_e, namely, the proportion of eddy loss which reflects the inhomogeneity of LV windings, are defined in Section IV.

B. Convective Heat Transfer Coefficients by CFD

In our previous work, an equivalent homogenization model is adopted by regarding the winding insulation layer and the conductor as a whole part [8]. This method ignores the distribution characteristics of the heat source of HV windings, which may cause larger temperature rise. The 1/64 3-D model considering the actual windings structure is established as

Authorized licensed use limited to: Hebei University of Technology. Downloaded on November 17,2022 at 09:36:45 UTC from IEEE Xplore. Restrictions apply.

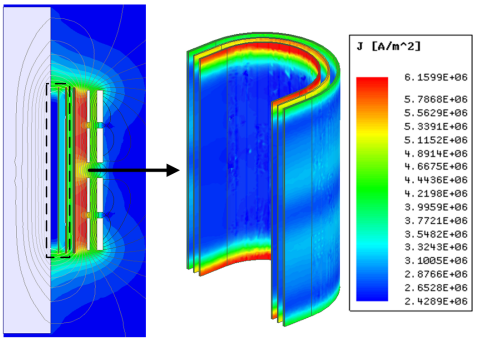


Fig. 3. Eddy current distribution of LV foil windings.

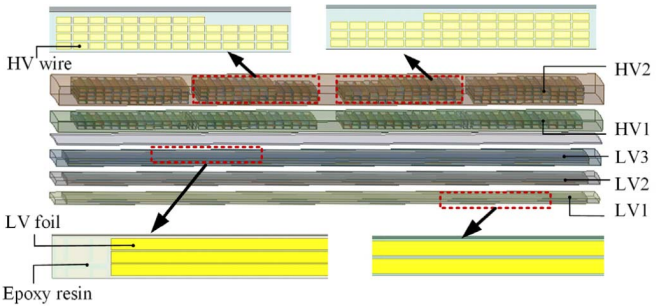


Fig. 4. Numerical simulation model of the dry-type transformer.

TABLE I
THERMAL CONDUCTIVITY

Material	Thermal conductivity [W/(m·K)]
copper	398
wire insulating paint	0.23
epoxy resin	0.276
insulating paper	0.21

shown in Fig. 4. The loss density distribution calculated by the electromagnetic field is imported into CFD through indirect coupling method.

When the dry-type transformer operates under natural convection condition, its heating windings cause air density change and convection cycle. The Boussinesq hypothesis is applicable due to Mach number (Ma) much less than 1. Considering thermal radiation effect between surfaces, the surface-to-surface (S2S) model is used to simulate thermal radiation effect. The thermal conductivity of the material is shown in Table I.

The distributions of temperature and velocity under natural convection at rated operation are shown in Figs. 5 and 6. The air heated by windings rises due to the buoyancy force. Therefore, the temperature of the transformer windings increases along the upward axial direction. Because of larger electrical loss, the hottest spot is located at the top segment of HV2 windings. At the inlet, the air flows faster because of higher wall temperature and narrower cooling ducts. Then, the distribution of the air velocity tends to be stable for the fully developed turbulent boundary layer. When reaching the outlet, the air velocity increases because of the reduced sectional area of the air flow path.

By extracting convective heat transfer coefficients from CFD, the effect of thermal radiation and convection by core loss is considered. h of LV windings and HV windings along

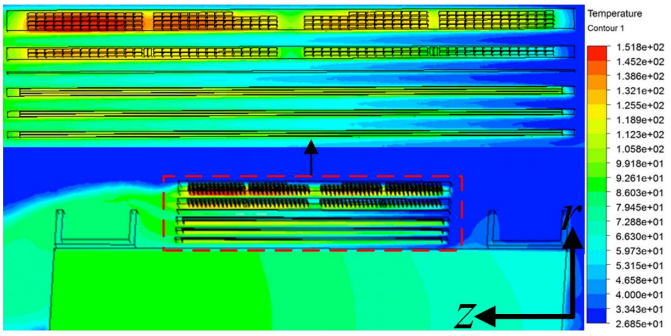


Fig. 5. Temperature distribution of LV and HV windings.

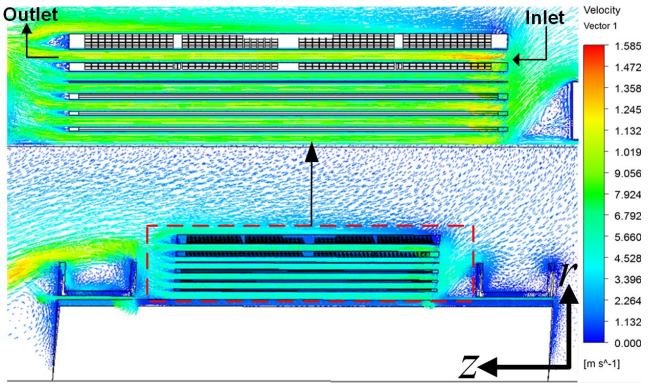


Fig. 6. Air velocity distribution of cooling ducts of windings.

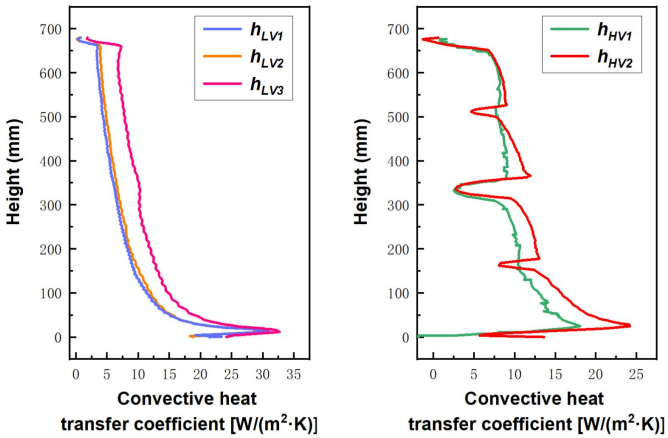


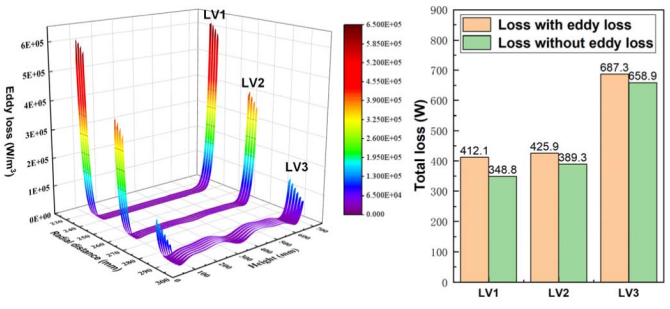
Fig. 7. Convective heat transfer coefficients of windings' surfaces. (a) h of LV windings. (b) h of HV windings.

the axial direction are shown in Fig. 7. h_i, namely, h at the ith region, is calculated by averaging over the ith region in Fig. 2.

In the surfaces of LV windings, h_{LV1}, h_{LV2}, and h_{LV3} reach a peak at the bottom of cooling ducts. The airflow climbs up with the rising temperature and the convective heat transfer coefficient decreased gradually. For HV windings, the overall trend of convective heat transfer coefficient is the same as that of LV windings, which decreases along the axial direction. However, because the heat source distribution of the HV windings is affected by their segmentation, h_{HV1} and h_{HV2} present a certain fluctuation locally.

According to Newton's cooling law in (4), the convective heat transfer coefficient h at the fluid–solid interface is determined by the temperature difference between the solid T_s and the reference temperature T_{ref} and by the heat flux

Authorized licensed use limited to: Hebei University of Technology. Downloaded on November 17,2022 at 09:36:45 UTC from IEEE Xplore. Restrictions apply.



(a) (b)

Fig. 8. Distribution of loss in LV windings. (a) Eddy loss in LV windings. (b) Total loss comparison in LV windings.

q_{conv} through the surface. Because the temperature difference between the surface and reference temperature gradually increases and the heat flux decreases along the axial direction, h shows a decreasing trend overall by (4):

$$h = \frac{q_{\text{conv}}}{(T_s - T_{ref})}. \tag{4}$$

At the end of the LV windings marked as 0–15 mm in Fig. 7, there is no internal heat source. The smaller heat flux only comes from the upper windings. In the part of 15–40 mm, the heat source is from the internal winding loss. Moreover, the significant eddy loss at the end caused by the leakage magnetic field in LV windings also has an impact on temperature rise. Consequently, the changing trend of h decreases along the axial direction overall and increases with the heat flux density locally.

IV. Calculation of Thermal Parameters

A. Calculation of Heat Source

As the heat source of the thermal network model, the winding loss comes from the dc and ac resistance loss. Due to the transverse leakage magnetic field, the eddy currents are induced in the ends of the foil coils, which lead to uneven distributions of loss among the LV windings shown in Fig. 8(a). Based on the electromagnetic FEM software, the total loss in LV windings is calculated as shown in Fig. 8(b). The parameter d_e is calculated in (5), which represents the proportion of eddy loss in each LV winding layer. P_e is the total eddy loss of LV windings and P_i is the eddy current loss of the region represented by node i. Due to the symmetry of eddy loss, d_e of nodes 1–6 is as listed in Table II

$$d_e = P_i / P_e. \tag{5}$$

B. Calculation of Thermal Resistances

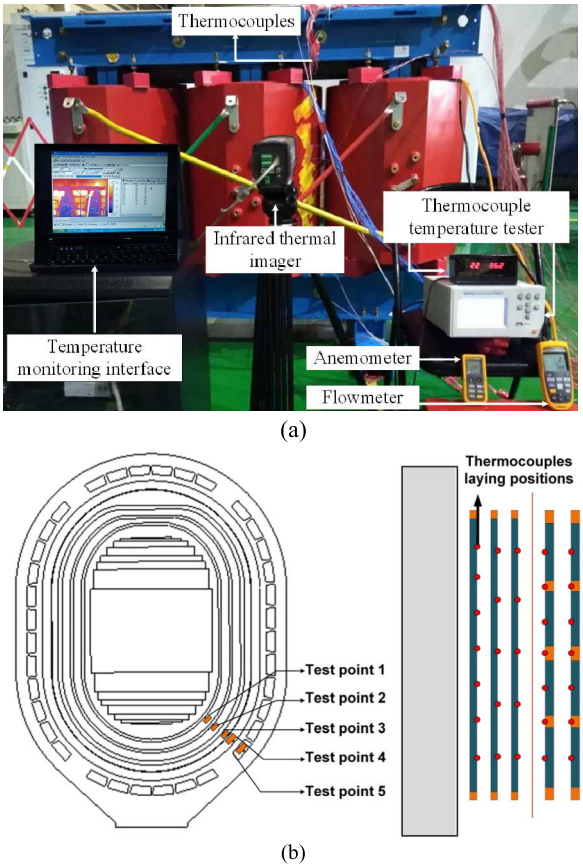
According to heat dissipation conditions, the thermal resistances contain conduction resistance, convection resistance, and radiant thermal resistance.

The thermal conduction resistance R_{cond} of the dry-type transformer is calculated by Fourier's law. Because the shape of windings is cylinder, the formula for cylindrical wall is adopted as follows:

$$R_{\text{cond}} = \frac{1}{2\pi\lambda} \ln \frac{r_2}{r_1} \tag{6}$$

TABLE II
Proportion of Eddy Current Loss in Each Region

Region number	Material	LV1	LV2	LV3
1	epoxy resin	--	--	--
2	copper	0.1689	0.1078	0.0576
3	copper	0.0221	0.0173	0.0198
4	copper	0.0095	0.0116	0.0223
5	copper	0.0095	0.0117	0.0223
6	copper	0.0097	0.0109	0.0154



(a)

(b)

Fig. 9. Temperature measuring experiment. (a) Experimental platform of temperature rise. (b) Schematic of thermocouples' laying positions.

where λ is the thermal conductivity of cylindrical wall, and r_1 and r_2 are the inner and outer diameters of the cylindrical wall, respectively.

The calculation formula of the thermal transfer convection resistance R_{conv} is shown as follows, where h represents the convective heat transfer coefficient of the surface, and A is the surface area

$$R_{\text{conv}} = \frac{1}{hA}. \tag{7}$$

The accuracy of h directly affects R_{conv} and temperature distribution. The empirical formula was always adopted to calculate h [9]. However, the applicable conditions of these formulas were relatively simple, which cannot be adapted for complex heat dissipation conditions of dry-type transformers. Since h is affected by the internal structural dimension of windings, the asymmetry heat sources, and the buoyancy lift

Authorized licensed use limited to: Hebei University of Technology. Downloaded on November 17,2022 at 09:36:45 UTC from IEEE Xplore. Restrictions apply.

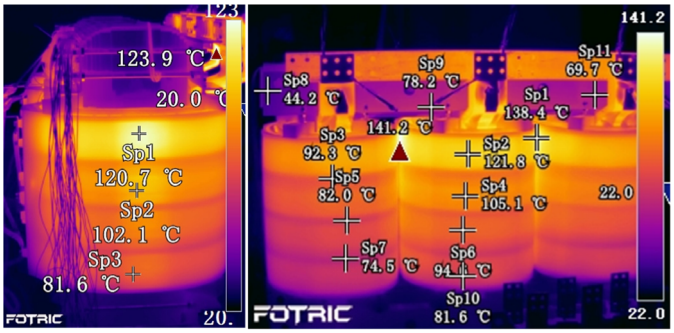
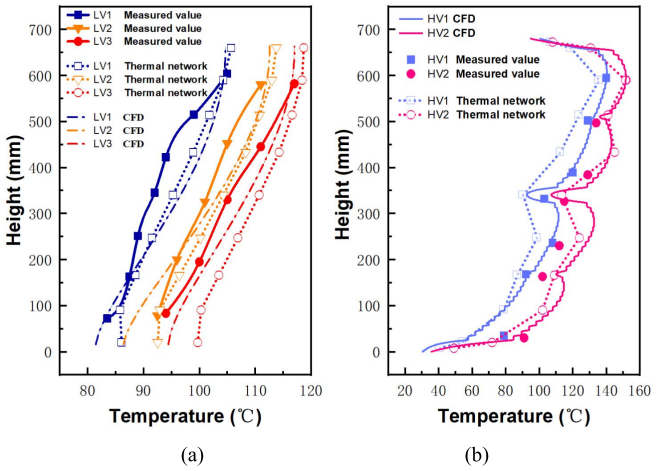


Fig. 10. Temperature measuring results by infrared imaging camera.



(a) (b)

Fig. 11. Comparison of temperature distribution by three methods. (a) LV windings' temperature. (b) HV windings' temperature.

of natural convection, it is obviously inaccurate to apply an averaged value for the whole plane. The parameter h extracted from CFD reflects the heat dissipation of each region accurately so that the temperature results are more precise and reliable.

When the dry-type transformer reaches heat dissipation equilibrium, the temperature in local areas can be up to more than 100 °C. The heat emitted to the environment by radiation is too considerable to be neglected. The radiant thermal resistance is related to the absolute temperatures of the two radiating surfaces T_1, T_2, the radius lengths r_1, r_2, the emissivities ε_1, ε_2, and the Stefan–Boltzmann's constant σ_b, which can be calculated by the Stephen–Boltzmann equation [9]. The radiant effect is considered by subtracting the radiant heat flux q_{rad} from the total winding loss

$$q_{\text{rad}} = \frac{\sigma_b\left(T_1^4 - T_2^4\right)}{(1/\varepsilon_1) + ((1-\varepsilon_1)/\varepsilon_2)(r_1/r_2)}. \tag{8}$$

V. Analysis of Experimental and Simulation Results

To verify the reliability of the thermal network model, the platform of the loading experiment is set up as Fig. 9. The 32-channel thermocouples are stuck on the surface of the HV and LV windings, and the overall temperature distribution is detected by infrared imaging camera. As shown in Fig. 10, the hottest temperature of windings' surfaces through the infrared imaging devices is 141.2 °C. The hottest spot is located in the highest disk of the outer HV windings with the temperature of 151.8 °C, which is in good agreement with the results of the thermal network model and CFD simulation in Fig. 11.

VI. Conclusion

According to the thermoelectric analogy effect, the thermal network is established. By coupling with CFD and FEM, the thermal parameters are obtained. The steady temperature of each region in dry-type transformer under natural convection is calculated. The following conclusions can be drawn.

1) Influenced by the windings' structure and the uneven heat source distribution, the axial convective heat transfer coefficients of transformer are not constant, whose evolving trend decreases along the axial direction but increases with local larger heat flux.
2) The hottest spot of the HV windings' surface is located at three-fourths of the height above the ground, the temperature of which is 151.8 °C at rated operation.
3) The thermal network method by coupling thermal parameters with FEM and CFD has more accurate precision than empirical formula. The experimental results verify the reliability of the established thermal network method.

Acknowledgment

This work was supported in part by the National Natural Science Foundation of China under Grant 51807048, Grant 51777055, and Grant 92066206 and in part by the Funds for Creative Research Groups of Hebei Province under Grant E2020202142.

References

[1] M. Xiao and B. X. Du, "Effects of high thermal conductivity on temperature rise of epoxy cast winding for power transformer," *IEEE Trans. Dielectr. Electr. Insul.*, vol. 23, no. 4, pp. 2413–2420, Aug. 2016.
[2] S. Zhu and X. Cai, "Transformer real-time reliability model based on operating conditions," *IEEE Trans. Energy Convers.*, vol. 33, no. 2, pp. 473–482, Jun. 2018.
[3] E. Rahimpour and D. Azizian, "Analysis of temperature distribution in cast-resin dry-type transformers," *Electr. Eng.*, vol. 89, no. 4, pp. 301–309, Feb. 2007.
[4] H.-M. Ahn, Y.-H. Oh, J.-K. Kim, J.-S. Song, and S.-C. Hahn, "Experimental verification and finite element analysis of short-circuit electromagnetic force for dry-type transformer," *IEEE Trans. Magn.*, vol. 48, no. 2, pp. 819–822, Feb. 2012.
[5] X. Yan, Y. Li, Z. Cheng, and C. Zhang, "Prediction of temperature rise for ventilated dry-type transformer by 3-D coupled magneto-fluid-thermal model," *Int. J. Appl. Electron.*, vol. 62, no. 4, pp. 725–735, Apr. 2020.
[6] G. R. Rodriguez, L. Garelli, M. Storti, D. Granata, M. Amadei, and M. Rossetti, "Numerical and experimental thermo-fluid dynamic analysis of a power transformer working in ONAN mode," *Appl. Thermal Eng.*, vol. 112, pp. 1271–1280, Feb. 2017.
[7] X. Bian and Y. Liang, "Circuit network model of stator transposition bar in large generators and calculation of circulating current," *IEEE Trans. Ind. Electron.*, vol. 62, no. 3, pp. 1392–1399, Mar. 2015.
[8] Y. Li, X. Yan, C. Wang, Q. Yang, and C. Zhang, "Eddy current loss effect in foil winding of transformer based on magneto-fluid-thermal simulation," *IEEE Trans. Magn.*, vol. 55, no. 7, pp. 1–5, Jul. 2019.
[9] F. P. Incropera, D. P. Dewitt, T. L. Bergman, and A. S. Lavine, *Fundamentals of Heat and Mass Transfer*. Beijing, China: Chemical Industry Press, 2007.

Authorized licensed use limited to: Hebei University of Technology. Downloaded on November 17,2022 at 09:36:45 UTC from IEEE Xplore. Restrictions apply.